Observation of the Reaction $\pi^- p \to p\bar{p}n$ at 8 GeV/c*

J. W. ANDREWS,† N. N. BISWAS, N. M. CASON, I. DERADO,‡ V. P. KENNEY,
J. A. POIRIER, AND W. D. SHEPHARD
Department of Physics, University of Notre Dame, Notre Dame, Indiana
(Received 14 June 1967)

We have observed the reaction $\pi^- p \to p\bar{p}n$ at 8 GeV/c with a cross section of 97 ± 26 μb. Because this reaction does not possess a distinctive topology in the bubble chamber which could distinguish it from the more frequent two-prong final states involving a nucleon and some number of pions, we have performed tests independent of the kinematic fitting process to confirm the presence of this reaction. These tests made use of the δ rays and secondary interactions produced by the negative tracks of our events. We have also investigated the possibility of various forms of contamination. Our final sample of events contains about 60% $p\bar{p}n$ final states and 40% background.

I. INTRODUCTION

THE reaction $\pi^- p \to p\bar{p}n$ has been searched for in a 40 000-picture exposure in the BNL 80-in. hydrogen bubble chamber at 8 GeV/c. This reaction belongs to a class of new reactions involving antibaryon production in meson-nucleon scattering, examples of which are beginning to be observed in a number of experiments.[1]

The study of this reaction is hampered by the fact that in addition to proceeding with a relatively small cross section, it does not possess a distinctive topology in the bubble chamber which could be used to distinguish it from the more frequent two-prong final states involving a nucleon and some number of pions. This contrasts with the more favorable situation in many strange-particle final states, where vees and kinks are present. We have felt, therefore, that tests independent of the kinematic fitting process must be used to establish whether the reaction does in fact occur with an appreciable cross section. The principal aim of this paper will be to demonstrate the presence of this reaction and to obtain a value for the cross section.

II. SELECTION OF EVENTS

The 80-in. hydrogen bubble chamber at Brookhaven National Laboratory was exposed to a beam[2] of 8.05 ±0.04 GeV/c π^- mesons. The film was scanned for all two-prong interactions; approximately 18 000 two-prong events in 40 000 pictures were measured. A total of 1003 events fitted the hypothesis $\pi^- p \to p\bar{p}n$ in GRIND with a χ^2 probability of at least 1%. These events were checked for consistency of both the positive and negative tracks with the predicted ionization; 591 events were rejected on this basis, leaving a sample of 412 events. Twelve of these had negative track momenta low enough to permit identification of the antiproton by ionization; these are discussed further in Appendix I.

As independent tests of the validity of the 412 fits, statistical analyses have been performed using the δ rays and secondary interactions produced by the negative tracks. The δ-ray analysis is based on the fact that the momentum distribution of δ rays is a function of the mass as well as the momentum of the particle producing them. The secondary interaction analysis depends on the fact that interactions are observed more frequently, and on the average with more charged outgoing tracks in $\bar{p}p$ collisions than in $\pi^- p$ events.

The outgoing negative tracks in the selected events were rescanned for secondary interactions and δ rays. The length of each negative track and the multiplicity of any secondary interaction were recorded. In addition, the radius of curvature of any δ ray having a diam of at least 1 cm on the scan table was measured, and its projected momentum q was calculated. In all, 81 δ rays and 29 secondary interactions were found.

The distribution for δ rays as a function of the projected momentum of the δ ray is derived in Appendix II. This distribution is, in general, different for antiprotons and pions of a given momentum k. If $\phi_f(k,q)$ is the distribution function assuming that a track has probability f of being an antiproton and $(1-f)$ of being a pion, then

$$\Phi_f(k,q) = f\Phi_p(k,q) + (1-f)\Phi_\pi(k,q),$$

where $\Phi_p(k,q)dq$ and $\Phi_\pi(k,q)dq$ are the probabilities per unit track length of producing a δ ray with projected momentum between q and $q+dq$ for antiprotons or pions of momentum k. Finally, a likelihood function is derived in Appendix II.

* Work supported in part by the National Science Foundation.
† National Aeronautics and Space Administration, predoctoral fellow. Present address: Yale University, New Haven, Connecticut.
‡ Present address: Stanford Liniar Accelerator Center, Stanford, California.
[1] M. L. Perl, L. W. Jones, and C. C. Ting, Phys. Rev. **132**, 1273 (1963); G. Bassompierre, Y. Goldschmidt-Clermont, A. Grant, V. P. Henri, B. Jongejans, R. L. Lander, D. Linglin, F. Muller, J. M. Perreau, A. Prokeš, R. Sekulin, and J. K. Touminiemi, Nuovo Cimento **48**, 589 (1967); Chih-Yung Chien, P. M. Dauber, D. J. Mellema, P. Schreiner, W. E. Slater, D. H. Stork, and H. K. Ticho, Bull. Am. Phys. Soc. **12**, 506 (1967); B. Forman, J. Berlinghieri, M. S. Farber, T. Ferbel, A. C. Melissinos, T. Yamanouchi, and H. Yuta, *ibid.* **12**, 540 (1967); J. Lach, J. Kim, T. Ludlam, J. Sandweiss, H. Taft, H. Foelsche, and H. Hahn, *ibid.*; B. C. Shen, R. W. Bland, A. Firestone, G. Goldhaber, J. A. Kadyk, B. Sheldon, and G. H. Trilling, *ibid.* **12**, 541 (1967).
[2] The AGS electrostatically separated beam 3 was operated in the unseparated mode. The beam has been described by I. Skillicorn and M. S. Webster, Brookhaven National Laboratory Bubble Chamber Group Report No. H10, 1962 (unpublished).

The secondary interactions produced by the negative tracks were measured and multivertex fits attempted. Multivertex fits were obtained in which the outgoing $\bar{p}$ underwent elastic scattering or produced additional pions without annihilating. No multivertex annihilation fit was obtained; this is not wholly unexpected, since antiproton annihilations usually produce more than one neutral particle.[3] Of the events in which the secondary interaction fit pion production without annihilation, it was possible in one case to identify uniquely by ionization the antiproton proceeding from the secondary vertex. This event is shown in Fig. 1. For the other multivertex fits, however, ionization information was of no help and the events were often ambiguous, with other possible interpretations.

Because of these uncertainties, a maximum-likelihood analysis was performed taking into account the frequency and topology of the secondary interactions. The analysis employed experimental values for the cross sections[4] for production of two-, four-, and six-prong interactions as a function of energy. The form of the likelihood function is given in Appendix III.

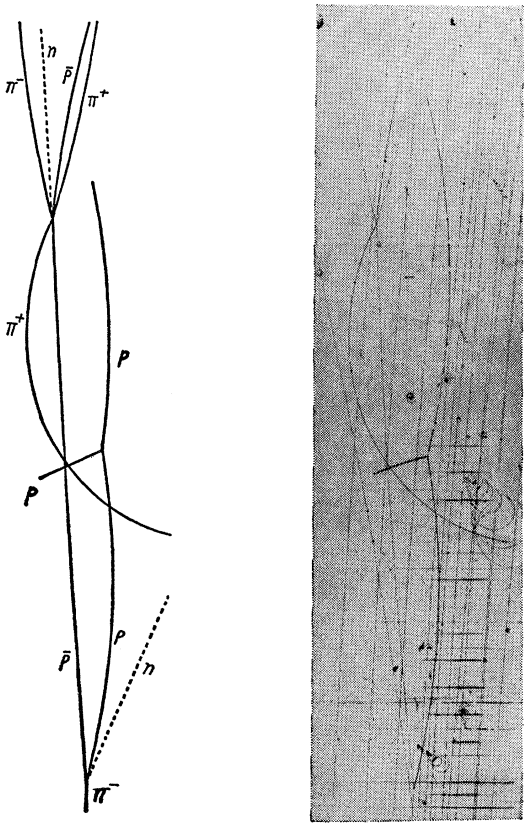

FIG. 1. An event fitting $\pi^- p \to p\bar{p}n$ at the primary vertex and $\bar{p}p \to \pi^+\pi^+\pi^-\bar{p}n$ at the secondary vertex of the negative track. The antiproton proceeding from the secondary vertex has a bubble density twice minimum. The multivertex fit was obtained with a χ^2 probability from GRIND of 0.95.

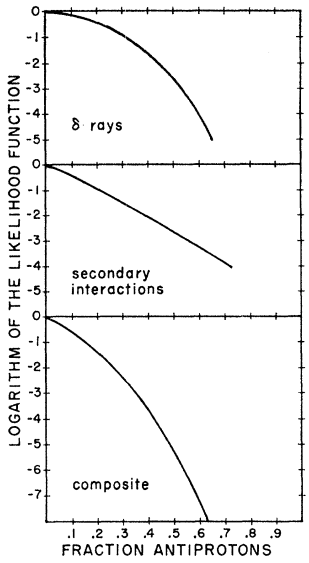

FIG. 2. Likelihood functions for events with both positive and negative track momenta greater than 2 GeV/c. Natural logarithms are used.

The results of these analyses are shown in Figs. 2 and 3. In each figure, the top curve is the logarithm of the likelihood function for the δ-ray analysis; the second curve is the logarithm of the likelihood function for the secondary interaction analysis; the bottom curve is a composite of the two. The curves in Fig. 2 refer to 163 events with both positive and negative track momenta in the lab greater than 2 GeV/c. The curves in Fig. 3 refer to 237 events having negative track momenta greater than 2 GeV/c but positive track momenta less than 2 GeV/c. We see that the likelihood functions are greatest for no antiproton production for the events with fast positive tracks. However, the likelihood functions peak between 50 and 70% antiproton production for the events with slow protons, with a best value of (60±16)% or 142 events.[5] This is

[3] We would expect to see about one annihilation into not more than one neutral among our secondary interaction measurements. This estimate takes into account our result for the number of antiproton events, the number of multivertex measurements successfully processed by HGEOM and GRIND, and the $\bar{p}p$ annihilation cross sections given by T. Ferbel, A. Firestone, J. Sandweiss, H. D. Taft, M. Gailloud, T. W. Morris, W. J. Willis, A. H. Bachman, P. Baumel, and R. M. Lea [Phys. Rev. **143**, 1096 (1966)].

[4] T. Ferbel, A. Firestone, J. Johnson, J. Sandweiss, and H. D. Taft, Nuovo Cimento **38**, 12 (1965); Saclay-Orsay-Bari-Bologna collaboration, Nuovo Cimento **35**, 1 (1965); **35**, 713 (1965); Aachen-Birmingham-Bonn-Hamburg-London-München collaboration, Nuovo Cimento **44A**, 530 (1966); K. Böckmann, B. Nellen, E. Paul, B. Wagini, I. Borecka, J. Diaz, U. Heeren, U. Liebermeister, E. Lohrmann, E. Raubold, P. Söding, S. S. Wolff, J. Kidd, L. Mandelli, L. Mosca, V. Pelosi, S. Ratti, and L. Tallone, *ibid.* **42A**, 954 (1966); R. Christian, A. R. Erwin, H. R. Fechter, F. E. Schwamb, S. H. Vegors, and W. D. Walker, Phys. Rev. **143**, 1105 (1966); T. Ferbel *et al.* (Ref. 3); F. E. James and H. L. Kraybill, Phys. Rev. **142**, 896 (1966).

[5] The number of secondary interactions observed in each of these samples of events is consistent with the known $\pi^- p$ and $\bar{p}p$ cross sections and the value of f obtained from the likelihood function.

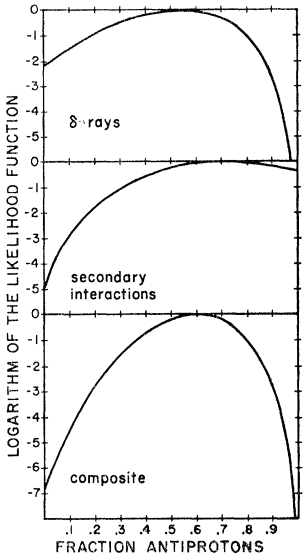

FIG. 3. Likelihood functions for events with positive track momentum less than 2 GeV/c and negative track momentum greater than 2 GeV/c. Natural logarithms are used.

in addition to the 12 events in which the negative track was uniquely identified as an antiproton by ionization.

As a check on the δ-ray and secondary interaction analyses, we performed the same analyses on 159 events with negative track momenta between 1 and 2 GeV/c, which were kinematically consistent with the antiproton hypothesis but were eliminated by bubble density measurements. Both likelihood functions peaked at 0% antiproton production, as expected.

III. CROSS SECTION

The most interesting result of this experiment is the determination of the cross section for the reaction $\pi^- p \to p\bar{p}n$ at 8 GeV/c. The numbers of events with their uncertainties for each of three groups of events are given in Table I. The quoted errors include statistical errors as well as errors due to the widths of the likelihood functions. In our data, one event corresponds to a cross section of 0.63 ± 0.03 μb.[6] The cross section for the reaction $\pi^- p \to p\bar{p}n$ is then 97 ± 26 μb.

IV. BACKGROUND

Since our analyses were statistical, it was not possible to select the examples of antiproton production on an event-by-event basis for our sample of 237 events with slow positive and fast negative tracks. In this section, therefore, we will try to determine the nature of the background. We also give evidence that our sample

TABLE I. Numbers of $\pi^- p \to p\bar{p}n$ events for various intervals of secondary-particle momenta.

Positive track momentum	Negative track momentum	Number of good $\bar{p}$ events
>2 GeV/c	>2 GeV/c	0_{-0}^{+17}
<2 GeV/c	>2 GeV/c	142_{-39}^{+37}
Unselected	<2 GeV/c	12 ± 4
All events		154_{-39}^{+41}

of negative tracks does not contain an appreciable amount of K^- contamination (note that our analyses assume that our tracks are all either $\bar{p}$ or π^-), and that we are not observing spurious antiprotons produced by $\bar{p}$ contamination in our beam.

We have tested the 237 events for the following alternative hypotheses in GRIND:

$$\pi^- p \to \pi^+\pi^- n \quad 22 \text{ events}, \quad (1)$$
$$\pi^- p \to p\pi^-\pi^0 \quad 21 \text{ events}, \quad (2)$$
$$\pi^- p \to pK^-K^0 \quad 54 \text{ events}, \quad (3)$$
$$\pi^- p \to K^+K^- n \quad 49 \text{ events}. \quad (4)$$

The number of fits to each hypothesis which could not be ruled out by ionization is shown at the right. A total of 69 events gave fits to one or more of these hypotheses; the numbers do not add to 69 because some of these events fitted more than one alternative hypothesis.

A total of 34 events fitted reaction (1) or (2). This represents an upper limit for contamination from these sources.

In order to determine whether we have contamination from reaction (3) or (4), we plotted the K^-K^0 effective mass for the 54 events fitting reaction (3) (Fig. 4), and the K^+K^- effective mass for the 49 events fitting reaction (4) (Fig. 5). The curve in Fig. 4 is phase-space normalized to 50 events expected for the reaction $\pi^- p \to pK^-K^0$, with the K^0 not decaying visibly in the chamber. This number was estimated by starting from a cross section of about 14 μb for the reaction $\pi^- p \to pK^-K_1^0$, with an observed K_1^0 decay, obtained from the data of Crennell *et al.* at 6 GeV/c.[7]

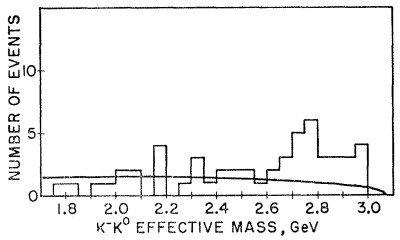

FIG. 4. K^-K^0 effective-mass distribution for 54 events which fit $\pi^- p \to pK^-K^0$ as well as $\pi^- p \to p\bar{p}n$. One event is off scale.

[6] From our fiducial volume and the number of beam tracks in our exposure we have determined that one event on the film corresponds to 0.463 ± 0.008 μb. This must be corrected for an $(86\pm2.5)\%$ scanning efficiency, $(14.5\pm0.4)\%$ unmeasurable events, $(3.9\pm0.1)\%$ systems loss and a 1% probability cut from GRIND. With these corrections we have a revised estimate of 0.63 ± 0.03 μb per event, in our sample.

[7] D. J. Crennell, G. R. Kalbfleisch, K. W. Lai, J. M. Scarr, T. G. Schumann, I. O. Skillicorn, and M. S. Webster, Phys. Rev. Letters **16**, 1025 (1966).

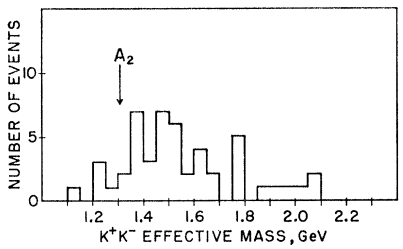

FIG. 5. K^+K^- effective-mass distribution for 49 events which fit $\pi^- p \to K^+K^- n$ as well as $\pi^- p \to p\bar{p}n$.

The events crowd the high end of the allowed effective-mass spectrum and greatly exceed the number expected in this range of effective mass for our entire exposure. On this basis we can rule out reaction (3) as a significant source of contamination. The K^+K^- mass spectrum (Fig. 5) for events fitting reaction (4) centers around lower values. The A_2 peak which might be expected for reaction (4) is not observed. This suggests a lack of K^+K^-n events in our sample, but is not conclusive since estimates indicate that the expected A_2 peak would not be statistically significant. It should be noted, however, that contaminations from reaction (4) can be significant only for events having positive track momentum greater than about 1.5 GeV/c, since below this momentum it is usually possible to distinguish between K^+ and proton by ionization. The δ-ray and secondary interaction analyses were repeated for events with an upper limit of 1.5 GeV/c rather than 2 GeV/c for the positive track momentum. For this sample, where contamination from reaction (4) cannot be large, no statistically significant change in the fraction of antiprotons was obtained.

Next we consider the question of $\bar{p}$ contamination in our beam. This has been estimated to be less than 1% for our exposure. However, to check the possibility that we are obtaining antiprotons in the final state from this source, we have tested in GRIND for hypotheses with an incident $\bar{p}$ and a $\bar{p}$ in the final state. Thirty-nine of the 237 events fit a hypothesis of this type; all these events were contained in the sample of 69 referred to above.

A special circumstance allows us to say more on this question. In general, the higher the circulating beam energy in the accelerator, the greater will be the ratio of $\bar{p}$ to π^- produced in a target. Our data were obtained in two separate runs with different AGS circulating beam energies for each run. The circulating beam energy was 19 GeV in the first run and 25.5 GeV in the second. The production angle for both runs was 7.5°. We have determined, using beam survey data from Brookhaven[8] and CERN,[9] that although 56% of our beam tracks were obtained in the later run, (81±5)% of our contaminating antiproton beam tracks occurred in that run.

If none of our events were produced by contaminating $\bar{p}$ tracks, we would expect 56% of our events to have come from the later run. If the $\bar{p}$ production we see were due entirely to incident antiprotons, we would expect (71±3)% of our events to have come from the second run. In fact, (57±3)% of the 237 events occurred in the later run. Also, of the 39 events fitting a hypothesis with both an incident and an outgoing antiproton, (51±8)% occurred in the later run. We conclude that incident antiprotons are not a major source of contamination.

Another possible source of background is final states with two or more neutral particles. The chief contributors to this form of background should be

$$\pi^- p \to p\pi^- + m\pi^0, \quad m \geq 2, \tag{5}$$

$$\pi^- p \to \pi^+\pi^- n + m\pi^0, \quad m \geq 1, \tag{6}$$

with reaction (5) dominating since most of the 237 events have a proton identified by ionization. As a check on this possibility, we have examined the plates in the downstream end of the 80-in. bubble chamber for production of pairs and showers by γ rays. If our events are mainly reaction (5), we expect to see the γ rays from decay of the π^0's.

For purposes of comparison, we have looked at the plates for samples of elastic scattering events and events in which a single π^0 is produced. The elastics give an estimate of the background due to misassociated γ rays produced elsewhere than at the vertex of the event in question. The single π^0 events give an estimate of the difference one neutral pion makes in the observed number of γ rays.

Our results are as follows. The elastic events gave an average of 0.58±0.09 conversions per event. In our sample of 237 events, we saw 0.67±0.08 conversions per event. For single π^0 events, we obtained 0.83±0.17 conversions per event. Thus, the result for the antiproton events falls between those for the elastic and the single π^0 events and, if anything, is closer to the elastic result. These results support the belief that we are not dealing mostly with events containing two or more π^0's.

V. CHARACTER OF THE $\pi^- p \to p\bar{p}n$ INTERACTION

In view of the presence of background, the exact amount and character of which is unknown, it is difficult to make definitive statements about the interaction. We point out some characteristics of the interaction, but the reader must realize that one should be cautious in drawing firm conclusions from these characteristics because of the background problem.

First we show the Dalitz plot of the events, together with the projections, in Fig. 6. The events tend to

[8] W. F. Baker, R. L. Cool, E. W. Jenkins, T. F. Kycia, S. J. Lindenbaum, W. A. Love, D. Lüers, J. A. Niederer, S. Ozaki, A. L. Read, J. J. Russell, and L. C. L. Yuan, Phys. Rev. Letters 7, 101 (1961).

[9] B. Jordan, CERN Report No. 65-14, 1965 (unpublished).

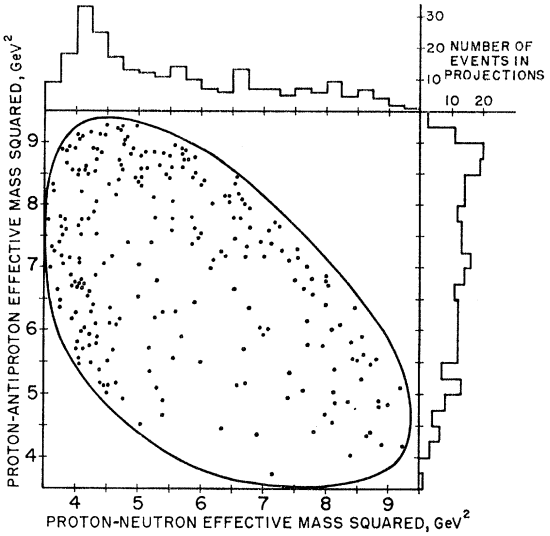

FIG. 6. Dalitz plot with projections for 249 events consistent with the hypothesis $\pi^- p \to p\bar{p}n$. Included are 237 events consisting of about 60% antiproton events and 40% background, plus 12 events containing antiprotons identified by ionization.

fall in either the low $\bar{p}n$ or the low pn effective-mass regions.

Second, we note that for most of the events, the momentum transfer from the target to the final-state proton is lower than the momentum transfer to either of the other outgoing particles. This suggests that the one-meson-exchange diagram of Fig. 7 may be important.[10]

Third, we show in Fig. 8 the distribution of the cosine of the Jackson angle θ, the angle between the incident π^- and the outgoing $\bar{p}$ in the $\bar{p}n$ center-of-mass system. This distribution is quite asymmetric with the antiproton going forward much more often than the neutron.

Finally, in Fig. 9, we show the Chew-Low plot of the $\bar{p}n$ effective mass versus the momentum transfer from the target to the outgoing proton. The peripheral nature of the reaction is quite evident, especially for the events with lowest $\bar{p}n$ effective mass.

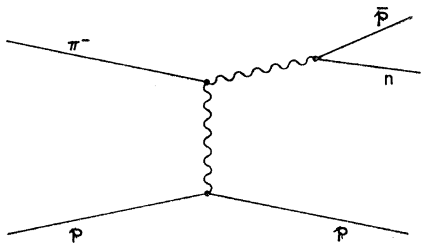

FIG. 7. One-meson-exchange diagram for the reaction $\pi^- p \to p\bar{p}n$. The wavy lines represent boson states of opposite G parity.

[10] F. Chilton, D. Horn, and R. J. Jabbur, Phys. Letters **22**, 91 (1966). A one-pion-exchange model for quark-antiquark production is applied to nucleon-antinucleon production.

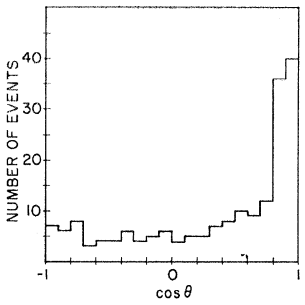

FIG. 8. Cosine of the Jackson angle, the angle between the incident π^- and the outgoing $\bar{p}$, in the $\bar{p}n$ center of mass. Plotted are 189 events for which the momentum transfer from incident to outgoing proton is less than the momentum transfer to either of the other two particles.

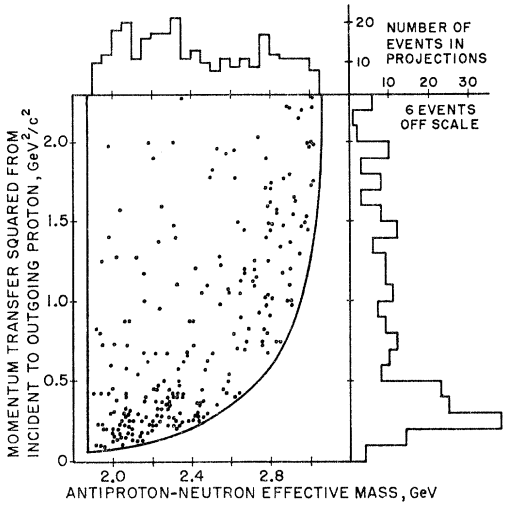

FIG. 9. Chew-Low plot of $\bar{p}n$ effective mass versus momentum transfer squared from incident to outgoing proton. Included are 237 events consisting of about 60% antiproton events and 40% background, plus 12 events containing antiprotons identified by ionization.

This experiment was made possible by the help and cooperation of the Shutt bubble chamber group and the alternating gradient synchrotron personnel of Brookhaven National Laboratory. We wish to thank Dr. R. Jabbur for helpful discussions and calculations. The efforts of Dr. E. H. Synn in collecting information necessary for the cross-section determination are acknowledged. We wish to thank J. B. Annable for assistance with the data analysis. We also express our appreciation to our scanning and measuring staff for their work on this experiment. The cooperation of the Notre Dame computing center is appreciated.

APPENDIX I: IDENTIFICATION OF ANTIPROTONS BY IONIZATION

Of our original 1003 GRIND fits to the reaction $\pi^- p \to p\bar{p}n$, 301 had negative track momenta less than 2 GeV/c. Of these, 12 were identified as antiprotons by ionization.

TABLE II. χ^2 values for events for which negative track ionization was measured with the microscope. The χ^2 is a measure of the consistency of the sample with being all pions.

Event sample	Positive track momentum	Negative track momentum	Other requirements	Number of events in sample	Number of identified $\bar{p}$ events	χ^2	Number of degrees of freedom	χ^2 probability
A	>2 GeV/c	<2 GeV/c		43	4	51	42	0.15
B	<2 GeV/c	<2 GeV/c	Positive track identified as proton	27	8	61	26	0.0001

For track momenta less than 1 GeV/c, track identification could usually be done by eye on the scan table. For tracks with momenta between 1 and 2 GeV/c, gap-length measurements were made with a microscope,[11] and fitted to a Poisson distribution via a maximum-likelihood calculation. The bubble density as a multiple of the bubble density for a minimum ionizing track was obtained, with statistical errors, assuming the beam track to be minimum ionizing.

We have considered the possibility that the 12 tracks identified as antiprotons could actually be only a statistical effect consistent with all the tracks in this momentum region (negative track momentum less than 2 GeV/c) being pions. We first estimated the size of the errors in bubble density measurements by considering all measurements for which a relative bubble density (secondary track to beam track) of less than 1.0 was obtained. These should be almost all pions, since the expected densities for antiprotons were of the order of 1.3 or more. Further, the expected densities for most of the tracks as pions were usually within 1 or 2% of 1.0. The histogram of bubble density measurements with results less than 1.0 was fitted to the left half of a Gaussian curve with a best value for the standard deviation of 0.158. This compares with an average statistical error of 0.12 due to Poisson statistics for these events. We may attribute the difference to effects such as pressure and temperature variations in the chamber, as a result of which a minimum ionizing track in the region of the chamber in which the secondary track is located may not have the same bubble density as the beam track.[12]

A χ^2 was defined as

$$\chi^2=(1/g^2)\sum_{i=1}^{n}(m_{\rm obs}-m_\pi)_i^2/\delta_i^2,$$

where $m_{\rm obs}$, m_π, and δ are the observed bubble density, pion bubble density, and statistical error for each event; g is the factor 0.158/0.12 which takes into account the fact that there are other errors besides the statistical errors due to the Poisson distribution. This χ^2 is a measure of the consistency of the measured bubble densities with the hypothesis that all the tracks are pions.

χ^2 values were calculated for two samples of events. Sample A consists of events for which the negative track bubble density was measured with the microscope and for which the positive track momentum was greater than 2 GeV/c. Sample B contains events for which the negative track was measured on the microscope and for which the positive track was identified as a proton by ionization. Table II shows the two samples and gives the χ^2 values obtained. The low χ^2 probability for sample B indicates that this sample of events is inconsistent with the hypothesis that all tracks are pions.

APPENDIX II. MAXIMUM-LIKELIHOOD CALCULATION FOR THE RELATIVE ABUNDANCE OF TWO TYPES OF PARTICLES IN A SET OF TRACKS, BASED ON δ-RAY PRODUCTION

A. Probability Distribution in Terms of δ-Ray Projected Momentum

If $\theta(\epsilon)d\epsilon$ is the probability per unit track length that a δ ray of energy between ϵ and $\epsilon+d\epsilon$ will be produced by an incident particle, and $P(\epsilon,q)dq$ is the probability that a δ ray of energy ϵ will have projected momentum between q and $q+dq$, then $\Phi(q)dq$, the probability per unit track length that a δ ray with projected momentum between q and $q+dq$ will be produced, is given by

$$\Phi(q)dq=dq\int\theta(\epsilon)P(\epsilon,q)d\epsilon. \qquad \text{(II1)}$$

By projected momentum, we mean the component of δ-ray momentum which lies in some plane containing the momentum of the particle producing δ rays. For the events which fit the reaction $\pi^- p \to p\bar{p}n$, the outgoing negative tracks dip very slightly, and hence lie close to the film plane. This fact allows us to measure the δ-ray momenta in the film plane at the scan table. We use the relation[13]

$$\theta(\epsilon)d\epsilon=2\pi N r_e^2 Z A^{-1}\rho mc^2\beta^{-2}(1/\epsilon^2-\beta/\epsilon\epsilon_{\rm max})d\epsilon, \qquad \text{(II2)}$$

[11] N. N. Biswas, I. Derado, K. Gottstein, V. P. Kenney, D. Lüers, G. Lütgens, and N. Schmitz, Nucl. Instr. Methods **20**, 135 (1963).

[12] N. N. Biswas, N. M. Cason, I. Derado, V. P. Kenney, J. A. Poirier, W. D. Shephard, and Sr. E. M. Clinton, G. N. S. H., in *Proceedings of the Thirteenth International Conference on High-Energy Physics, Berkeley* (University of California Press, Berkeley, California, 1967), p. 145.

[13] B. Rossi, *High Energy Particles* (Prentice-Hall, Inc., Englewood Cliffs, New Jersey, 1952), p. 15. We have included the density ρ in the equation to give $\theta(\epsilon)$ units of energy^{-1} length^{-1} rather than energy^{-1} mass^{-1} length^2.

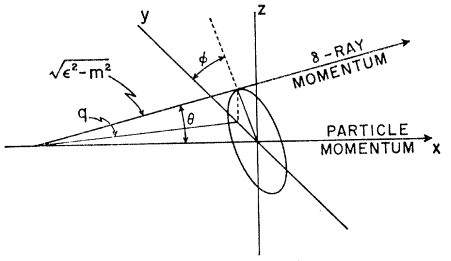

FIG. 10. Kinematics of δ-ray production. The polar angle θ is a function of the δ-ray energy ϵ and the relativistic velocity β of the particle which produces the δ ray.

where N is Avogadro's number; m and r_e are the mass and classical radius of the electron; Z, A, and ρ are the charge number, mass number, and density of the material through which the particles pass; βc is the velocity of the δ-ray-producing particle; and $\epsilon_{\max}$ is the maximum possible δ-ray energy.

Assuming that δ rays come off at all azimuthal angles with equal probability, the probability $P(\epsilon,q)$ will be greatest for those ranges of q which spread over a large range of ϕ angles (Fig. 10). In fact

$$P(\epsilon,q) \propto |d\phi/dq|. \tag{II3}$$

With the proper normalization

$$P(\epsilon,q) = (2/\pi)\frac{q}{\{[q^2-(\epsilon^2-m^2)\cos^2\theta][\epsilon^2-m^2-q^2]\}^{1/2}}, \tag{II4}$$

where θ and ϕ are the polar and azimuthal angles of the δ-ray momentum. From energy-momentum conservation in δ-ray production it follows that

$$\cos^2\theta = (\epsilon-m)^2/\beta^2(\epsilon^2-m^2). \tag{II5}$$

Substituting Eqs. (II2), (II4), and (II5) into (II1), and setting the limits of integration such that ϵ takes on only values which are compatible with a given q, we obtain

$$\Phi(q)dq = 4Nr_e^2ZA^{-1}\rho mc^2\beta^{-2}qdq \times\int_{q^2+m^2}^{m+\beta q}(1/\epsilon^2-\beta/\epsilon\epsilon_{\max}) \times\frac{d\epsilon}{\{[q^2-(\epsilon-m)^2/\beta^2][\epsilon^2-q^2-m^2]\}^{1/2}}, \tag{II6}$$

which involves an elliptic integral.

B. The Likelihood Function

Before constructing the likelihood function we need the following result. The probability of getting a δ ray with momentum between some minimum projected momentum q_0 and the maximum $q^{\max}$ in a short track length ΔL is

$$\Delta L\int_{q_0}^{q^{\max}}\Phi(q)dq. \tag{II7}$$

Then the probability of not getting such a δ ray in a finite length L is

$$\lim_{\Delta L\to 0}\left(1-\Delta L\int_{q_0}^{q^{\max}}\Phi(q)dq\right)^{L/\Delta L} = \exp\left[-L\int_{q_0}^{q^{\max}}\Phi(q)dq\right]. \tag{II8}$$

Following Sec. II we use for $\Phi(q)$ a composite distribution function $\Phi_f(k,q)$ defined as follows: Let $\Phi_p(k,q)dq$ and $\Phi_\pi(k,q)dq$ be the probabilities per unit track length of producing a δ ray with projected momentum between q and $q+dq$ for antiprotons or pions of momentum k. Thus, $\Phi_p(k,q)$ and $\Phi_\pi(k,q)$ are just the function $\Phi(q)$ derived in part A evaluated for different values of β. Let f be the probability that the track is an antiproton. Then

$$\Phi_f(k,q) = f\Phi_p(k,q)+(1-f)\Phi_\pi(k,q). \tag{II9}$$

Using the distribution function $\Phi_f(k,q)$, we construct the likelihood function for δ-ray production on one track of length L (see Fig. 11). If we divide the track into small lengths ΔL and the allowed range of δ-ray momenta into small units Δq, we can write the probability for n δ rays to occur in their observed unit lengths and momentum intervals as

$$\mathcal{P} = \exp\left[-(L-n\Delta L)\int_{q_0}^{q^{\max}}\Phi_f(k,q)dq\right] \times(\Delta q\Delta L)^n\prod_{i=1}^{n}\Phi_f(k,q_i), \tag{II10}$$

where q_i is the momentum of the ith δ ray.

If we now have m tracks, where the jth track has momentum k_j, length L_j, and number of δ rays n_j with projected momenta q_{ij} (with i running from 1 to n_j),

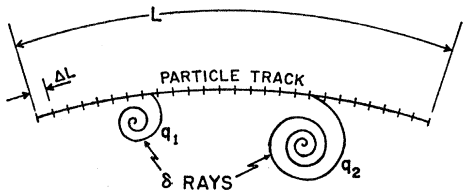

FIG. 11. Division of a track into small lengths ΔL for the construction of the likelihood function [Eq. (II13)].

then we can write

$$\mathcal{P}=\prod_{j=1}^{m}\left\{\exp\left[-(L_j-n_j\Delta L)\int_{q_0}^{q_j^{\max}}\Phi_f(k_j,q)dq\right]\times(\Delta q\Delta L)^{n_j}\prod_{i=1}^{n_j}\Phi_f(k_j,q_{ij})\right\}. \quad \text{(II11)}$$

Taking the logarithm,

$$\mathcal{L}\equiv\ln\mathcal{P}=-\sum_{j=1}^{m}L_j\int_{q_0}^{q_j^{\max}}\Phi_f(k_j,q)dq+\Delta L\sum_{j=1}^{m}n_j\int_{q_0}^{q_j^{\max}}\Phi_f(k_j,q)dq+\sum_{j=1}^{m}n_j\ln(\Delta q\Delta L)+\sum_{j=1}^{m}\sum_{i=1}^{n_j}\ln\Phi_f(k_j,q_{ij}). \quad \text{(II12)}$$

We note that this function has one free parameter, f, and that the others are all fixed in a given experiment. We want to find the value of f between 0 and 1 which maximizes the likelihood function. If we take ΔL and Δq small but nonzero, the second term is small with respect to the first. The third, although it becomes large and negative, does not depend upon f, and hence can be ignored. We use, then, for the logarithm of the likelihood function

$$\mathcal{L}=-\sum_{j=1}^{m}L_j\int_{q_0}^{q_j^{\max}}\Phi_f(k_j,q)dq+\sum_{j=1}^{m}\sum_{i=1}^{n_j}\ln\Phi_f(k_j,q_{ij}). \quad \text{(II13)}$$

APPENDIX III. STATISTICAL ANALYSIS OF SECONDARY INTERACTIONS

Consider a track of length L and momentum k. Let p_2, p_4, p_6, π_2, π_4, and π_6 be the probabilities per cm of track for producing a 2-, 4-, or 6-prong secondary if the track is an antiproton or pion, respectively. The probability of not getting a secondary over the length of the track is

$$e^{-L[f(p_2+p_4+p_6)+(1-f)(\pi_2+\pi_4+\pi_6)]}, \quad \text{(III1)}$$

where f is the probability that the track is an antiproton.[14a] If there is a secondary at the end of the track (in the last length ΔL) we must multiply this probability by a term $\Delta L[fp_2+(1-f)\pi_2]$ if the secondary is a two prong, and with subscripts 4 or 6 for four- or six-prong secondaries, respectively. If we have m tracks, some of which produce secondaries, we can write for the probability

$$\mathcal{P}=\prod_{j=1}^{m}e^{-L_j[f(p_{2j}+p_{4j}+p_{6j})+(1-f)(\pi_{2j}+\pi_{4j}+\pi_{6j})]}\times\prod_{2\text{ prongs}}\Delta L[fp_{2j}+(1-f)\pi_{2j}]\prod_{4\text{ prongs}}\Delta L[fp_{4j}+(1-f)\pi_{4j}]\prod_{6\text{ prongs}}\Delta L[fp_{6j}+(1-f)\pi_{6j}], \quad \text{(III2)}$$

where we have added the subscript j to those quantities which vary from track to track. Taking the logarithm,

$$\mathcal{L}\equiv\ln\mathcal{P}=-\sum_{j=1}^{m}L_j[f(p_{2j}+p_{4j}+p_{6j})+(1-f)(\pi_{2j}+\pi_{4j}+\pi_{6j})]+\sum_{\substack{\text{all}\\ \text{secondaries}}}\ln\Delta L+\sum_{2\text{ prongs}}\ln[fp_{2j}+(1-f)\pi_{2j}]+\sum_{4\text{ prongs}}\ln[fp_{4j}+(1-f)\pi_{4j}]+\sum_{6\text{ prongs}}\ln[fp_{6j}+(1-f)\pi_{6j}]. \quad \text{(III3)}$$

We note that the first term is just f times N_p, the number of secondary interactions one would expect if all the tracks were antiprotons, plus $(1-f)$ times N_π, the number of secondary interactions one would expect if all the tracks were pions. N_p and N_π can be calculated for a given sample of events from the lengths of the tracks and the experimental cross sections for $\bar{p}p$ and $\pi^- p$ scattering into the different topologies.[4] The second term does not depend on f and may be ignored. In the terms involving sums ever secondaries, the secondary interaction probabilities are proportional to the cross sections. Substitution of cross sections for probabilities in $\mathcal{L}$ is equivalent to adding a constant, which will not affect our result. Hence, we use for the logarithm of the likelihood function

$$\mathcal{L}=-fN_p-(1-f)N_\pi+\sum_{2\text{ prongs}}\ln[f\sigma_{2p}+(1-f)\sigma_{2\pi}]+\sum_{4\text{ prongs}}\ln[f\sigma_{4p}+(1-f)\sigma_{4\pi}]+\sum_{6\text{ prongs}}\ln[f\sigma_{6p}+(1-f)\sigma_{6\pi}]. \quad \text{(III4)}$$

[14a] *Note added in proof.* It has been pointed out to us that expression (III1) is only an approximation to the correct probability distribution in that it does not take into account the variation in f with track length caused by the different π^- and $\bar{p}$ total cross sections. We have evaluated the likelihood functions using the correct expression

$$f\exp[-L(p_2+p_4+p_6)]+(1-f)\exp[-L(\pi_2+\pi_4+\pi_6)]$$

and find that the correction to the likelihood functions is negligible (the value of f and its error change by less than 1%). We would like to thank Professor U. Kruse for pointing this out to us.

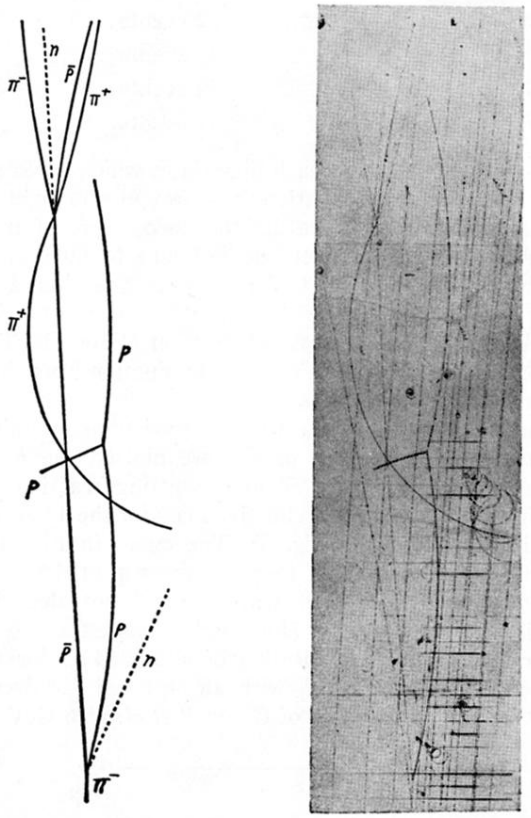

FIG. 1. An event fitting $\pi^- p \rightarrow p\bar{p}n$ at the primary vertex and $\bar{p}p \rightarrow \pi^+\pi^+\pi^-\bar{p}n$ at the secondary vertex of the negative track. The antiproton proceeding from the secondary vertex has a bubble density twice minimum. The multivertex fit was obtained with a χ^2 probability from GRIND of 0.95.